

pp. 489 and 797.

<sup>4</sup>Mott and Massey, Ref. 3, pp. 618–621.

<sup>5</sup>A. Sommerfeld, Ann. Physik **11**, 257 (1951).

<sup>6</sup>J. D. Jackson and H. Schiff, Phys. Rev. **89**, 359

(1953).

<sup>7</sup>R. H. Bassel and E. Gerjouy, Phys. Rev. **117**, 749 (1960).

<sup>8</sup>R. A. Mapleton, Phys. Rev. **130**, 1839 (1963).

PHYSICAL REVIEW A

VOLUME 3, NUMBER 3

MARCH 1971

## Measurement of Ionization Growth Rates in H<sub>2</sub> at High $E/p$

A. Buffa, G. Malesani, and G. F. Nalesso

*Centro Gas Ionizzati, Consiglio Nazionale delle Ricerche,*

*Università di Padova – c/o Istituto di Elettrotecnica e di Elettronica, Padova, Italy*

(Received 14 April 1970; revised manuscript received 26 October 1970)

Ionization growth rates of hydrogen, in the range of  $E/p$  between 100 and 10 000 V/cm Torr are presented. They have been deduced from microwave measurements of electron densities in a ring-shaped discharge, produced by a uniform magnetic field linearly increasing in time. The experimental conditions are described and the meaning of the obtained data is discussed as well as compared with the more usual results in a straight uniform electric field. At  $E/p \leq 1000$ , the obtained values of  $\beta/p$ , where  $\beta$  is the ionization growth rate, increase with  $E/p$  and are in good agreement both with theory and earlier experiments. At  $E/p > 2000$ , on the contrary,  $\beta/p$  decreases with increasing  $E/p$  as suggested by theory, but not yet measured experimentally. The maximum of  $\beta/p \approx 1.3 \times 10^9$  sec Torr<sup>-1</sup> corresponds to  $E/p \approx 2000$ .

### INTRODUCTION

The growth rate  $\beta$  for the ionization of H<sub>2</sub> in a uniform electric field  $E$  and its dependence on  $E/p$ , are well-known for  $E/p$  up to 1000 V/cm Torr. Figure 3, which will be discussed in due course, shows a comparison of the values of  $\beta/p$  calculated by the theory<sup>1</sup> and the experimental results both in straight<sup>2,3</sup> and annular geometry.<sup>4</sup> For  $E/p$  of the order of a few thousand, on the contrary, only theoretical calculations,<sup>5,6</sup> which deduce the ionization-growth rates from simplified models, are available.

The rate  $\beta$ , defined by the equation  $n(t) = n_0 e^{\beta t}$ , describes the growth of the electron density  $n(t)$  in a spatially homogeneous time-dependent ionization process. The measurements here described were taken by means of a microwave interferometer in the closed electrodeless geometry of an induced ring discharge. In such a configuration, uniformity is assured along the lines of the applied electric field  $E$ , while the influence on the measured growth rates of the field and density gradients perpendicular to  $E$  will be discussed. This paper deals with the experimental apparatus and the results obtained with values of  $E/p$  between 100 and 10 000 V/cm Torr. Furthermore, the influences of the axial magnetic field and of the electric field curvature are discussed here.

### EXPERIMENTAL LAYOUT

The experimental apparatus shown in Fig. 1 is similar to those used for “ $\theta$ -pinch” experiments. A single-turn coil  $C$  (40 cm long, 18 cm in diameter)

is energized at time  $t = 0$  by connecting it to a pre-charged condenser bank. The Pyrex vacuum tube  $T$ , coaxial with the coil, can be a single-walled cylinder (radius  $R = 2.5$ – $4$  cm), or a double-walled vessel (two coaxial cylinders, delimiting an annular region of thickness  $\Delta R = 1$ – $1.5$  cm). A cylindrical graphite screen  $S$  (resistivity  $\approx 100$   $\Omega$ /square) assures that the conservative component of the electric field (due to the feed-point discontinuity of the coil<sup>7,8</sup>) is eliminated within a few nanoseconds.<sup>9</sup> The required initial electron density  $n_0$  is obtained by means of a very weak axial predischARGE. Oscillograms (Fig. 2) of the coil voltage  $V$  and of the magnetic field  $B$ , show that between 30 and 300 nsec,  $V$  is nearly constant, while  $B$  increases linearly. Therefore, the electric field  $E$  inside the Pyrex tube is azimuthal, nearly constant in time, and proportional to the distance  $r$  from the axis,  $E = \frac{1}{2} \dot{B} r$ , with an upper limit  $E(R) = \frac{1}{2} \dot{B} R$  near the tube wall.  $\dot{B}$  can be varied between  $5 \times 10^5$  and  $10^6$  T/sec. It has been verified, with a differential probe,<sup>10</sup> that  $V$  and  $B$  are not perturbed by the gas current during the observation time.

The horns  $A$ - $A$  (Fig. 1) are part of the measuring path of an 8-mm microwave interferometer. This is inside a screening room, so that the electrical noise is always negligible at the sensitivity employed. The microwave beam goes through the holes  $H$ - $H$  and is focused on the tube axis by the dielectric lenses  $L$ - $L$ . The resulting propagation vector is radial and therefore parallel to the electron-density gradients; the electric vector of the wave is polarized in the direction of the main mag-

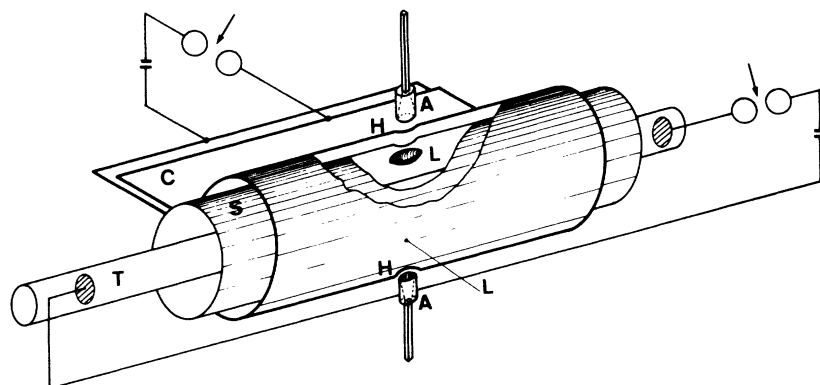


FIG. 1. Experimental layout.

netic field.

#### MEASUREMENT OF IONIZATION GROWTH RATES

In the present experiment, the density  $n$  is a function not only of time, but also of the radial distance  $r$  from the axis, because the ionization growth rate depends on the local strength of  $E$ , which is proportional to  $r$ . At any time the smallest electron density is on the axis while the largest  $\hat{n}(t)$  is at a proper value of  $r \leq R$ .

The phase shift of the interferometer,  $\Delta\phi(t)$ , is equivalent to that produced by a single slab of uniform electron gas, with density  $\hat{n}(t)$  and thickness  $D(t)$ , given by<sup>11</sup>

$$\Delta\phi(t) = \frac{2\pi D(t)}{\lambda_0} \left[ 1 - \left( 1 - \frac{\hat{n}(t)}{n_c} \right)^{1/2} \right], \quad (1)$$

where  $n_c$  is the cutoff density. Equation (1) shows that a direct measurement of  $D(t)$  can be obtained from the phase shift up to the cutoff time, because then  $\hat{n}$  is known and equal to  $n_c$ . By means of the  $z$  predischage, the initial electron density can be varied, and the cut-off reached at different times. In this way the diagram of  $D(t)$ , for each set of the parameters  $(\dot{B}, R, \Delta R, p)$ , can be evaluated. The diagram of  $D(t)$  thus obtained can be approximately used also at lower densities, since the radial density distribution does not depend on the actual density values, but only on the local values of  $\beta$ . This is true, provided the maximum ion density is much less than the total gas density.

If the function  $D(t)$  is known, the ratio of the maximum electron densities  $\hat{n}_1$  and  $\hat{n}_2$  at two different times  $t_1$  and  $t_2 = t_1 + \Delta t$  in the same discharge, can be determined from the corresponding phase-shifts:

$$\frac{\hat{n}_2}{\hat{n}_1} = \frac{\Delta\phi_2 D_1}{\Delta\phi_1 D_2} \left( \frac{1 - (\Delta\phi_2 \lambda_0)(4\pi D_2)^{-1}}{1 - (\Delta\phi_1 \lambda_0)(4\pi D_1)^{-1}} \right). \quad (2)$$

This immediately gives the ionization growth rate in the region of maximum electron densities  $\beta = \ln(\hat{n}_2/\hat{n}_1)(\Delta t)^{-1}$ .

The main error affecting this method is due to the thickness evaluation; its absolute value can be

measured with an accuracy of the order of  $\pm \frac{1}{4}\lambda_0$ , but in the chosen working conditions, the ratio  $\hat{n}_2/\hat{n}_1$  depends mainly on the thickness variation during  $\Delta t$ , which can be evaluated with a much better accuracy. The resulting error in  $\beta$  has been estimated to be less than  $\pm 10\%$  in the most unfavorable condition (double-walled vessel and  $p = 10$  mTorr).

The  $H_2$  filling pressures have been measured by means of a McLeod vacuum gauge. The impurity contents have been evaluated at  $p \geq 50$  mTorr from spectral line intensities and have been found to be less than 1%. At the lowest pressure (10 mTorr) we can reasonably expect that they should not be over 5%.

#### EXPERIMENTAL RESULTS

All the growth rate measurements started from  $t_1 > 40$  nsec, when the applied voltage has already reached its plateau; the incremental times  $\Delta t$  were of the order of  $1/\beta$  and the electron densities of the order of  $10^{12} \text{ cm}^{-3}$ . The obtained values of  $\beta$  for each set of the experimental parameters  $(\dot{B}, R, \Delta R, p)$  were well reproducible within the experimental error.

With filling pressures between 100 mTorr and 1 Torr, for different values of  $\dot{B}$  and  $R$ , measurements have been taken in the range of  $E(R)/p$  between 100 and 1000 V/cm Torr. The obtained  $\beta/p$  values were a unique function of  $E(R)/p$  and not separately of  $E(R)$  and  $p$ . Furthermore, the measured equivalent thickness (of order of  $\lambda_0$ ) and the values of  $\beta/p$  were the same in the single- and double-walled vessels. This fact indicates that

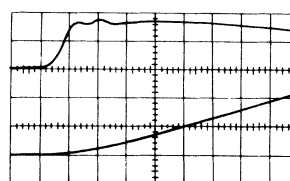


FIG. 2. Waveforms of the coil voltage (upper beam) and of the magnetic field on its axis (lower beam). Time base: 40 nsec/div; Vertical sensitivity: upper beam 10 kV/div; lower beam 0.08 T/div.

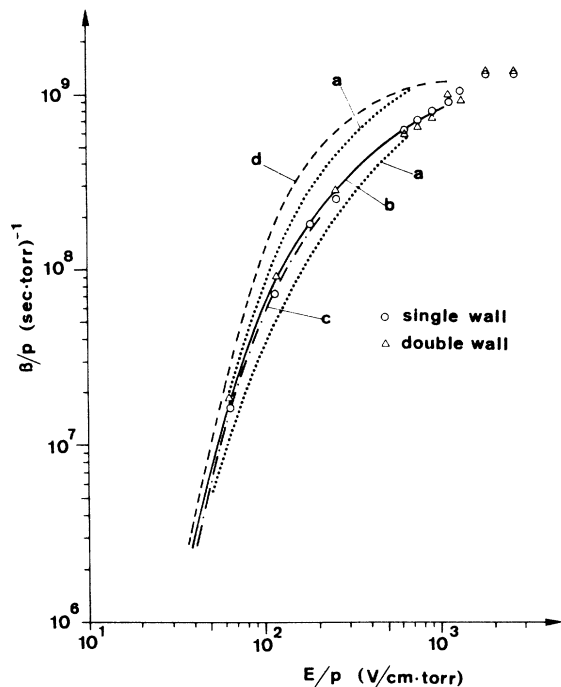


FIG. 3. Growth rates in  $H_2$  with  $E/p$  between 100 and 1000 V/cm Torr. Curves a-a represent the upper and lower limits of theoretical calculations for dc electric field (Ref. 1). Other curves represent experimental results: b in straight dc electric field (Ref. 3); c in microwave field, results referred to the effective electric field (Ref. 2); d in dc toroidal electric field (Ref. 4). Points are the present experimental results in dc toroidal electric field.

the ionization grows mainly near the outer tube wall, where both the electric field and  $\beta$  are higher. Therefore the measured values of  $\beta/p$  may be as-

cribed to the electric field strength  $E = E(R)$  (Fig. 3).

At the lowest filling pressures ( $p = 10\text{--}50$  mTorr), values of  $E(R)/p$  up to 10000 have been attained. The measured values of  $\beta/p$  in the single-walled vessel seem nearly independent of  $E/p$ , but the equivalent thickness of the ionized layer is much larger than in the previous cases and therefore a large range of electric fields appears to be responsible for the ionization. In a double-walled vessel, on the contrary, ionization is allowed only in the annular region  $\Delta R$ ; the measured total equivalent thickness of the ionized layer is again of the order of  $\lambda_0$ . The growth rates  $\beta$ , at constant pressure, are clearly a decreasing function of the applied electric field and, for each coil voltage, the  $\beta/p$  values decrease with the filling pressure. The  $\beta/p$  reported in Fig. 4 are the averages of several values measured in a vessel with  $R = 3.5$  cm and  $\Delta R = 1.5$  cm; the dispersion is always less than 10%. The same values of  $\beta/p$  plotted in Fig. 8 versus  $E(R)/p$ , appear a unique function of this variable. The decrease of  $\beta/p$  for  $E(R)/p > 2000$  cannot be observed in the single-walled vessels because in that case there is always a layer where  $E$  corresponds to the maximum ionization growth rate.

#### DISCUSSION OF THE RESULTS

In order to understand the physical meaning of the measured growth rates, the main aspects of the motion of free charged particles in a uniform axial magnetic field  $B = \dot{B}t$ , with cylindrical symmetry, must be recalled. A particle of mass  $m$  and charge  $e$ , born at a time  $t_b$  with zero velocity and at a distance  $r_b$  from the axis, is considered. Its free motion can be usefully divided in two phases.

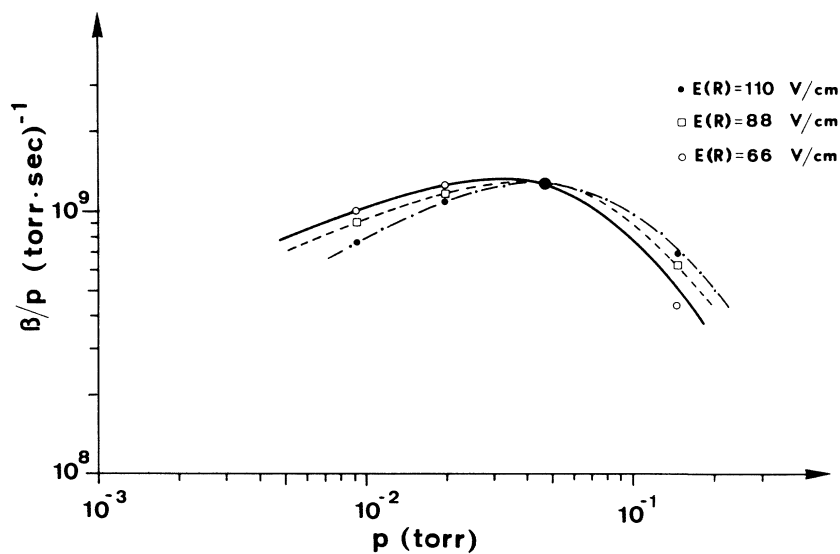


FIG. 4. Plot of the growth rates measured in  $H_2$  versus  $p$ , with  $E(R)/p \geq 1000$  V/cm Torr,  $R = 3.5$  cm and  $\Delta R = 1.5$  cm.

During the first phase the acceleration is nearly constant and azimuthal, because the electric force prevails over the Lorentz and the centrifugal forces. In the second phase, where the relative increase of the magnetic field during a cyclotron period is small ( $\dot{B}/B \ll eB/m = \omega$ ), the reverse is true and the kinetic energy of the particle remains proportional to the magnetic field and therefore increases linearly with time.<sup>12</sup> The time  $t_a = t_b + \Delta t_a$  when the electric force equals the Lorentz force may be assumed as the end of the first phase<sup>13</sup> - from the motion equation, one can deduce  $\Delta t_a \approx [\dot{\omega}(t_b + \Delta t_a)]^{-1}$ , where  $\dot{\omega} = e\dot{B}/m$ . Numerical integration of the exact equations<sup>14</sup> shows (Figs. 5 and 6) that after  $\Delta t_a$  the speed of the particle is only several percent less than  $(e/m)E\Delta t_a$ , and the distance from the axis remains practically equal to  $r_b$ . Afterwards  $t_a$ , the trajectory of the particle, progressively deviates from the electric field line: It spirals towards the axis (Fig. 6) and the kinetic energy oscillates around a mean value that linearly increases with time. The time scale of the motion is proportional to  $\sqrt{m}$ ; therefore the electrons move inwards faster than the positive ions, and a radial electric field due to charge separation appears. For electron densities higher than  $10^8$ - $10^9$  cm<sup>-3</sup>, this space-charge field is strong enough to force

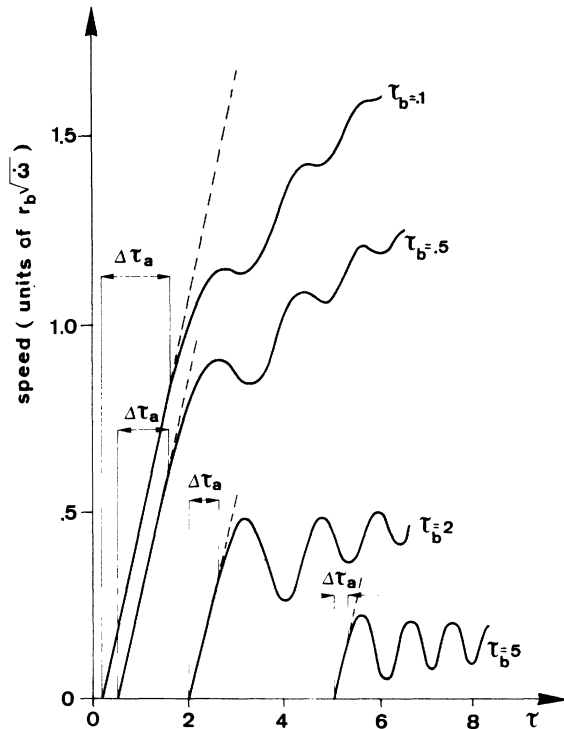


FIG. 5. Speed diagrams of charged particles in uniform magnetic field  $B = \dot{B}t$  (plotted vs the reduced time  $\tau = t\sqrt{\dot{\omega}}$ ), for different birth times  $\tau_b$ .  $\Delta\tau_a \approx (\tau_b + \Delta\tau_a)^{-1}$  is the time interval of constant acceleration.

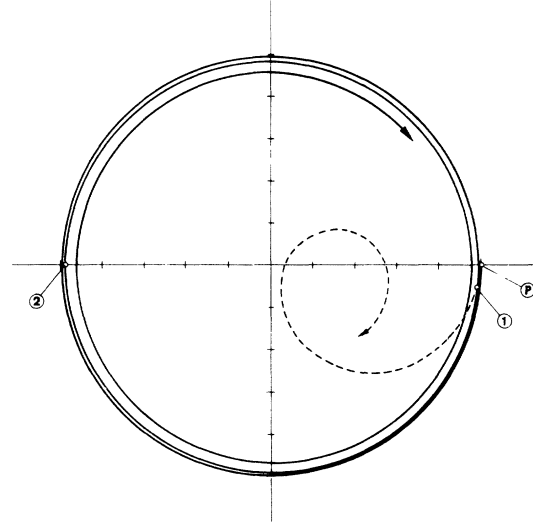


FIG. 6. Typical trajectories of electrons in axial uniform magnetic field  $B = \dot{B}t$ , born immediately after the zero of  $B$  and at point  $P$ . Dashed and continuous lines are the trajectories without and with strong space charge; points 1 and 2 are the positions reached at the end of the respective constant-acceleration phases.

electrons and ions to move radially together. If this condition is included into the motion equations for the electrons, their constant acceleration phase is magnified by a factor  $(m_i/m_e)^{1/2}$  and becomes  $\Delta t_a \approx [\dot{\omega}_h(t_b + \Delta t_a)]^{-1}$ , where  $\dot{\omega}_h$  is the time derivative of the hybrid frequency  $eB/(m_i m_e)^{1/2}$ . Furthermore, the electron trajectories make many turns around the axis with a slow radial deflection (Fig. 6) so that any initial azimuthal inhomogeneity in electron density is soon averaged. The growth rate measurements here described have been done immediately after the voltage rise, when  $B$  is small and  $\Delta t_a$  large. In Fig. 7 the "total collision time"  $1/\nu_c$  in  $H_2$  is compared with  $\Delta t_a$  at various birth times. The initial electron densities were high enough to always assure the space-charge effect.

For  $p \geq 50$  mTorr [which corresponds to  $E(R)/p$  up to 2000 V/cm] the measured growth rates are clearly due to electrons colliding with neutrals before the end of  $\Delta t_a$ . The motion of electrons is then much like the motions in a uniform and constant electric field. This fact may explain the good agreement, pointed out in Fig. 3, between the presently measured  $\beta/p$  for  $E(R)/p$  up to 1000 and those found by other authors.

For  $p < 50$  mTorr [i. e.,  $E(R)/p > 2000$ ], a fraction of the electrons collides with the inner wall before it collides with gas particles, owing to the radial displacement. Since these electrons reach the wall together with the ions (owing to the space-charge effect), they can easily recombine, thus reducing the measured growth rate. A "pure volume" ion-

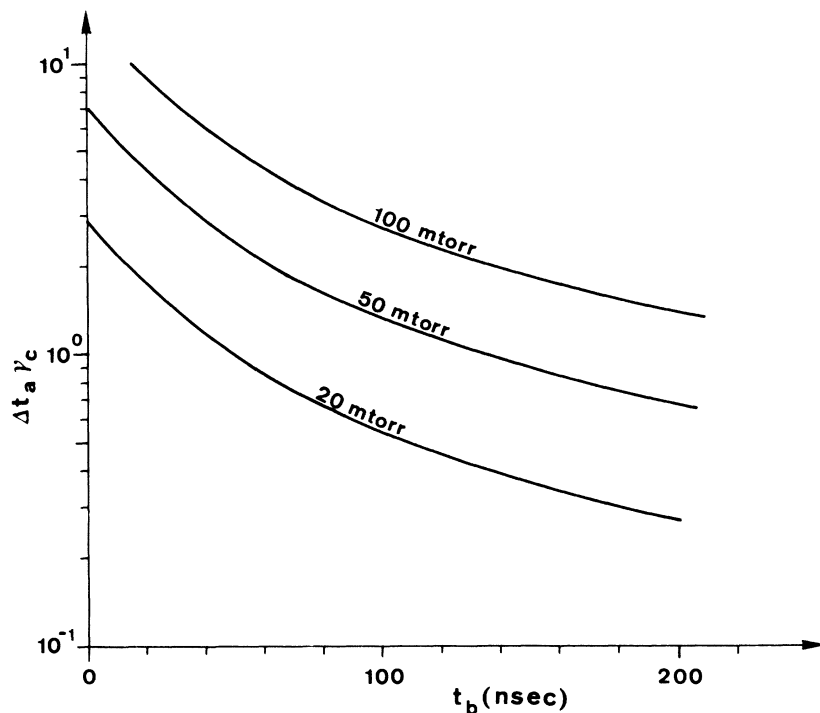


FIG. 7. Comparison of the constant acceleration time  $\Delta t_a \approx [\omega_h(t_b + \Delta t_a)]^{-1}$  with the total collision frequency  $\nu_c$  in  $H_2$ .  $\nu_c/p = 4.8 \times 10^9$  (sec Torr) $^{-1}$ ;  $\dot{B} = 6.4 \times 10^5$  T/sec.

ization rate  $\beta^*$  may be calculated, assuming that all these electrons are lost:  $\beta^* = \beta[1 + (\beta t_f)^{-1}]$ , where  $t_f$  is the time required to cross  $\Delta R$ .<sup>14</sup> This is clearly an overestimation of the losses, but does not change the decreasing bend of the curve at high  $E/p$  (Fig. 8). Diffusion to the walls, because of collisions with gas particles, should not appreciably affect the growth rates at these high  $E/p$ .<sup>1</sup> Moreover the results are practically the same both with  $\Delta R = 1$  cm and  $\Delta R = 1.5$  cm, confirming that wall effects are not important in the present experimental conditions; lower values of  $\beta$  have been observed only with  $\Delta R \leq 0.5$  cm. An opposite correction, diminishing the measured  $\beta$  by some percent, should be made if impurity effects are considered.

Theoretical models<sup>5,6</sup> indicate that the average electron energy, on which the growth rate depends, reaches a steady-state value only after several ionization times  $1/\beta$ . In the experiments performed, the equilibrium is certainly reached in the pressure range down to 60–80 mTorr. At lower pressures this condition was not strictly satisfied, but within the maximum allowed shift in the observation time (of the order of  $1/\beta$ ) no changes in the measured values were noticed, therefore they should not be far from the actual steady-state values.

#### CONCLUSIONS

The present experimental conditions, and therefore the measured growth rates, are those currently occurring in the low-pressure plasma pro-

duction by means of  $\theta$  pinch. In the double-walled vessel the measured values of  $\beta/p$  appear as a unique function of  $E/p$  in the whole explored range. This function increases for low values of  $E/p$  and decreases at high values. The maximum, of the order of  $1.3 \times 10^9$  (sec Torr) $^{-1}$  is attained for  $E/p \approx 2000$  V/cm Torr. It has been pointed out in

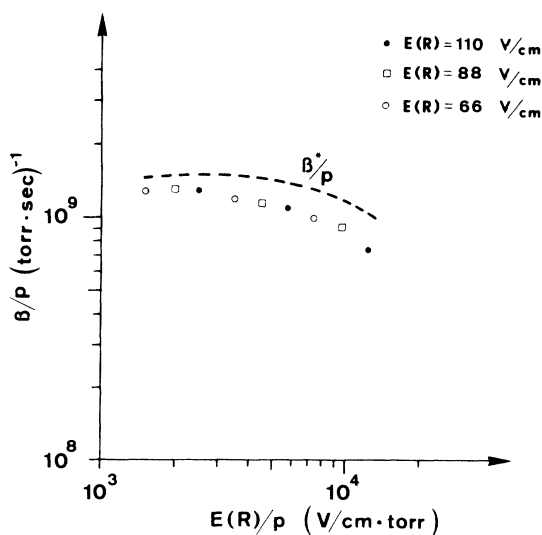


FIG. 8. Plot of the measured growth rates at the higher  $E/p$  vs  $E(R)/p$  ( $R = 3.5$  cm;  $\Delta R = 1.5$  cm).  $\beta^*$  is an overestimated correction of the measured  $\beta$ , to take into account the losses at the inner wall.

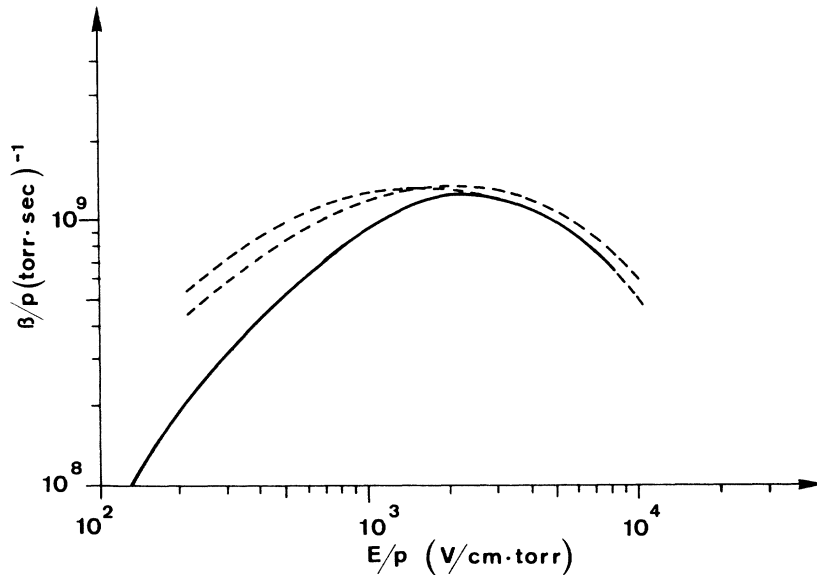


FIG. 9. Comparison of present results with theoretical calculations of Gerjuoy and Stuart, Ref. 5 (applicable only to the very high  $E/p$  range and in a steady-state condition). The solid line correspond to the measurements, the dashed lines to the calculations.

the previous description, that in the double-walled vessel, the ionization grows mainly in a thin layer. With  $E(R)/p \leq 1000$  this layer is near the outer wall where  $E$  is maximum, because  $\beta$  increases with  $E$ . With  $E(R)/p > 2000$ , on the contrary, the ionization grows mainly where  $E$  is minimum (inner wall). The continuous line of Fig. 9 corresponds to the actual values of  $E/p$  in the ionized layer.

The experimental configuration approximately realizes the spatially homogeneous conditions required for a correct definition of  $\beta$ . While in the ideal conditions of a uniform electric field the particle acceleration is constant between collisions; in our case this is true only when  $\nu_c \Delta t_a > 1$ . At the lowest pressures, the particle acceleration is reduced after a time  $\Delta t_a$  by the magnetic field: for the same values of  $E/p$  the mean electron energy is therefore smaller than in the ideal case. The negative slope of the ideal  $\beta/p$  curve should then be

more pronounced than in our measurements. It may be worthwhile to mention, in connection with this problem, that also in a straight electric field the observed drift velocities of electrons at high  $E/p$  (measurements<sup>3</sup> in  $H_2$  with  $E/p \leq 2000$  V/cm Torr) are smaller than those evaluated from the classical collision frequency  $\nu_c$  and comparable to those attainable in our case within the interval  $\Delta t_a$  alone.

We believe that the results here presented may be taken as a first experimental evidence of the decrease of  $\beta/p$  at high  $E/p$  suggested by theoretical models<sup>5</sup>: The agreement is good in the validity range of the quoted theory (Fig. 9).

#### ACKNOWLEDGMENT

We express our thanks to Dr. G. Rostagni and our appreciation for his constant interest in this work and his careful revision of the manuscript.

<sup>1</sup>G. A. Baraff and S. J. Buchsbaum, Phys. Rev. **130**, 1007 (1963).

<sup>2</sup>W. B. Cottingham and S. J. Buchsbaum, Phys. Rev. **130**, 1002 (1963).

<sup>3</sup>H. Schlumbohm, Z. Physik **182**, 317 (1965); **184**, 492 (1965).

<sup>4</sup>H. Beerwald, Report Jül/480/PP of Institut für Plasmaphysik der Kern Forschungs Anlage, Jülich, D. B. R., 1967 (unpublished).

<sup>5</sup>E. Gerjuoy and G. N. Stuart, Phys. Fluids **3**, 1008 (1960).

<sup>6</sup>K. G. Müller, Z. Physik **169**, 432 (1962).

<sup>7</sup>G. Malesani, E. Mazzucato, G. Rostagni, and B. Scimemi *Proceedings of the Fifth International Conference on Ionization Phenomena in Gases, Munich, 1961*, edited by H. Maeckner (North-Holland, Amsterdam, 1962),

Vol. II, p. 2138.

<sup>8</sup>G. Malesani, in *Proceedings of the Sixth International Conference of Ionization Phenomena in Gases, Paris, 1963*, edited by P. Hubert (SERMA, Paris, 1964), Vol. II, p. 581.

<sup>9</sup>M. R. Barrault and J. McCartan, Brit. J. Appl. Phys. **16**, 1535 (1965).

<sup>10</sup>T. S. Green, Nucl. Fusion **2**, 92 (1962).

<sup>11</sup>M. A. Heald and C. B. Wharton, *Plasma Diagnostics with Microwaves* (Wiley, New York, 1965).

<sup>12</sup>W. P. Allis, in *Handbüch der Physik*, edited by S. Flügge (Springer-Verlag, Berlin, 1956), Vol. 21, p. 383.

<sup>13</sup>R. Chodura Z. Naturforsch. **19a**, 679 (1964).

<sup>14</sup>A. Buffa, G. Malesani, G. Rostagni, and G. Zangiro-lami, Report UPe 70/07 of Istituto di Elettrotecnica e di Elettronica, Padova, Italy, 1970 (unpublished).